Ultrafast Exciton Dynamics in Silicon Nanowires

ARTICLE *in* JOURNAL OF PHYSICAL CHEMISTRY LETTERS · MARCH 2012

Impact Factor: 7.46 · DOI: 10.1021/jz201597j

6 AUTHORS, INCLUDING:

Jian-An Huang
The University of Hong Kong
13 PUBLICATIONS **148** CITATIONS
SEE PROFILE

Zhang Jin
Huainan Normal University
62 PUBLICATIONS **823** CITATIONS
SEE PROFILE

THE JOURNAL OF PHYSICAL CHEMISTRY Letters

Letter

pubs.acs.org/JPCL

Ultrafast Exciton Dynamics in Silicon Nanowires

Damon A. Wheeler,[†] Jian-An Huang,[‡] Rebecca J. Newhouse,[†] Wen-Feng Zhang,[‡] Shuit-Tong Lee,*[,‡] and Jin Z. Zhang*[,†]

[†]Department of Chemistry and Biochemistry, University of California, Santa Cruz, California 95064, United States

[‡]Center of Super-Diamond and Advanced Films (COSDAF) & Department of Physics and Materials Science, City University of Hong Kong, Hong Kong SAR, China

Supporting Information

ABSTRACT: Ultrafast exciton dynamics in one-dimensional (1D) silicon nanowires (SiNWs) have been investigated using femtosecond transient absorption techniques. A strong transient bleach feature was observed from 500 to 770 nm following excitation at 470 nm. The bleach recovery was dominated by an extremely fast feature that can be fit to a triple exponential with time constants of 0.3, 5.4, and ~75 ps, which are independent of probe wavelength. The amplitude and lifetime of the fast component were excitation intensity-dependent, with the amplitude increasing more than linearly and the lifetime decreasing with increasing excitation intensity. The fast decay is attributed to exciton−exciton annihilation upon trap state saturation. The threshold for observing this nonlinear process is sensitive to the porosity and surface properties of the sample. To help gain insight into the relaxation pathways, a four-state kinetic model was developed to explain the main features of the experimental dynamics data. The model suggests that after initial photoexcitation, conduction band (CB) electrons become trapped in the shallow trap (ST) states within 0.5 ps and are further trapped into deep trap (DT) states within 4 ps. The DT electrons finally recombine with the hole with a time constant of ~500 ps, confirming the photophysical processes to which we assigned the decays.

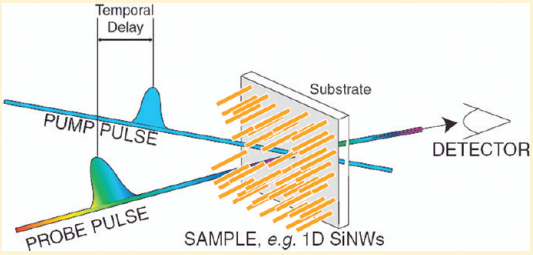

SECTION: Dynamics, Clusters, Excited States

Nanostructured silicon has been the focus of recent interest since the discovery of its photoluminescent (PL) properties in 1990 by Canham.[1] It has potential applications in biological sensors,[2−4] field-effect transistors (FETs),[5−7] integrated logic circuits,[8] and photodynamic therapy.[9] Bulk silicon is known to be an indirect bandgap semiconductor[10] with weak PL. Because of this, quantum confinement effects are thought to be the cause of PL in silicon nanocrystals.[11−14] Surface effects have also been suggested to play an important role in the PL of nanostructured Si.[15−18] For instance, cathode luminescence and time-resolved PL spectroscopy have shown that luminescence in silicon nanowires (SiNWs) is due to interface states and surface radiative recombination centers located at the interface of the silicon core and the SiO_2 cladding layer.[19,20]

Ultrafast dynamics of excitons and charge carriers in nanostructured silicon have been studied, particularly in relation to its PL properties. Fast carrier thermalization times of ~150 fs via phonon emission have been seen before[21] along with intraband relaxation times of ~240 fs.[22] Silicon grains showed a fast decay component of 400 fs, attributed to the quenching of the interior exciton radiative recombination by carrier trapping,[23] while another study found a 500 fs component attributed to nanocrystallite defect scattering.[24] Other investigations observed a femtosecond component that was proposed to be due to molecule-like silicon complexes or clusters in the material.[25,26] Additionally, a feature that decayed in ~3 ps was monitored and found to be dependent on the porosity of the sample.[27]

One-dimensional (1D) silicon structures, such as nanowires, in particular hold interest over zero-dimensional (0D) structures due to their potential advantage of better charge transport along the long axis, which is important for certain applications such as nanoscale transistors,[6,28,29] sensors,[4,30] power sources[31] and battery anodes.[32] Despite this, little work has been done on the ultrafast dynamics of excitons and charge carriers in 1D porous SiNWs.

In this work, we studied the early time exciton dynamics of 1D SiNWs using ultrafast laser techniques. The ultrafast exciton dynamics are dominated by an extremely fast feature that can be fit with a triple exponential with fast and slow components. The threshold for observing the fast component (~300 fs), attributed to nonlinear exciton−exciton annihilation, was found to be dependent on pump power. The slower and pump power-independent decay, ~5 ps, is attributed to exciton relaxation from the shallow trap (ST) to the deep trap (DT). A much slower and small amplitude delay with a time constant on the order of ~75 ps is likely associated with recombination from

Received: December 5, 2011
Accepted: March 1, 2012
Published: March 1, 2012

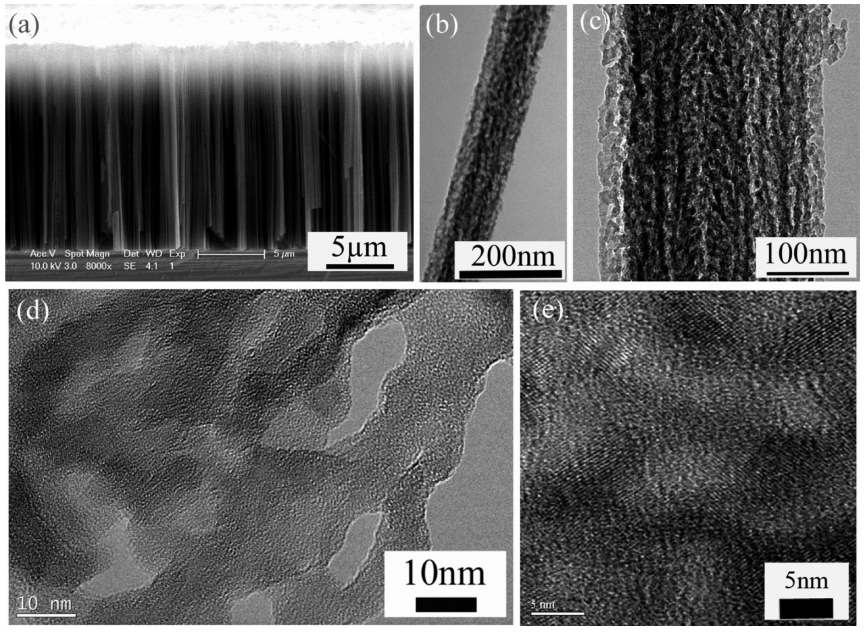

Figure 1. (a) SEM and (b–e) TEM images of 1D SiNWs that show vertical alignment (a) as well as a mesoporous structure (b–e).

the DT to the valence band (VB) and is related to the weak PL observed. Finally, a kinetic modeling scheme was developed that supports the experimental decay profiles and mechanism and helps account for the main features of the experimental dynamics.

Figure 1 shows scanning electron microscopy (SEM) and transmission electron microscopy (TEM) images of the 1D SiNWs. Figure 1a reveals vertically aligned SiNWs with a length of approximately 15 μm and an average diameter of ~150 nm. The SiNWs shown in Figure 1b–e exhibit a high degree of surface roughness, porosity, and polycrystallinity and are covered by a cladding layer of SiO_2. High-resolution TEM (HRTEM) shows the irregularly shaped pores of the SiNWs, which are 5 to 10 nm in size. Image analysis indicates an average porosity of ~18% for the SiNWs.

Figure 2 shows the PL spectrum (red line) of the SiNWs, which displays weak near-infrared (NIR) emission with peaks centered at 732 and 800 nm that are in good agreement with previously reported spectra.[33−35] The small peak at 732 nm arises from the SiNWs' thin oxide coating, while the broad peak at 805 nm is likely due to the emission from the localized excitation in the porous sample.[33] Figure 2 also displays the ultraviolet–visible (UV–vis) spectrum (blue line) of the SiNWs that shows a broad absorption ranging from 300 to 800 nm with a peak centered near 460 nm. The spectrum of the SiNWs matches well with previously reported spectra for NWs and shows a long absorption tail persisting beyond 800 nm attributed to the indirect nature of the bangap.[36]

Figure 3 is a three-dimensional (3D) plot of the transient time decay profile (in ps) for the SiNWs following excitation at

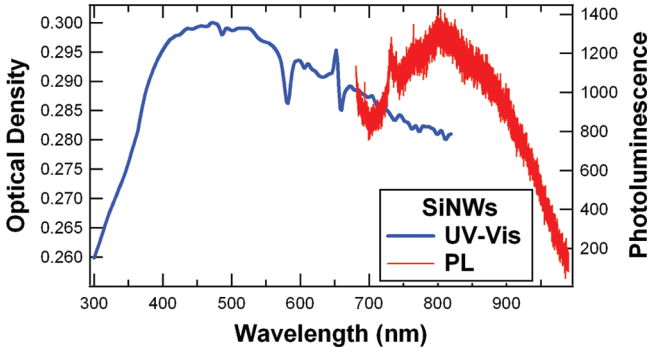

Figure 2. Electronic absorption (blue line) and fluorescence (red line, with λ_{ex} = 514.5 nm) spectra.

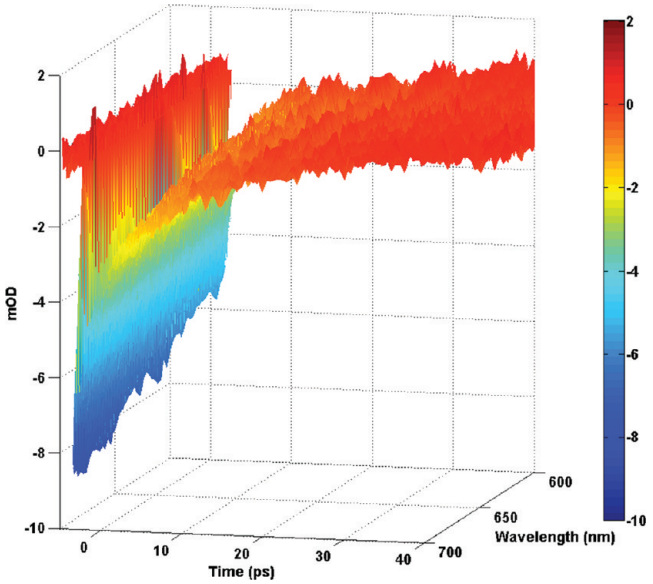

Figure 3. 3D transient bleach relaxation traces of 1D SiNWs at probe wavelengths spanning 600–700 nm following a 470 nm, 200 nJ/pulse pump.

470 nm (maintained at a pulse energy of 200 nJ/pulse) at probe wavelengths of 600–700 nm. A pulse-width-limited (<180 fs) transient bleach is followed by an exponential fast recovery (~0.3 ps), a slow exponential recovery (~ 5 ps), and a third small amplitude, slower (~75 ps) exponential recovery. Similar decay profiles have been observed for other pump

dx.doi.org/10.1021/jz201597j | J. Phys. Chem. Lett. 2012, 3, 766–771

powers, including the notion that the amplitude and time constant for the fast component change with pump power. The transient bleach data showed that the observed time constants are independent of probe wavelength, while their amplitudes vary with probe wavelength, indicating that the transient species has a broad spectrum and the spectral intensity is wavelength dependent. Figure 3 also shows that the maximum intensity of the signal is larger for redder probe wavelengths, increasing by ~60% over a span of 100 nm.

Figure 4 shows that as the pump power was decreased from 200 nJ/pulse to 125, 80, and 40 nJ/pulse, the amplitude of the

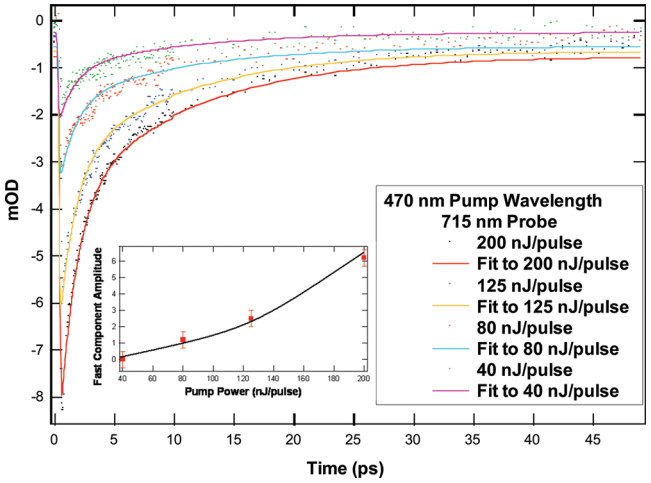

Figure 4. Transient bleach relaxation traces of 1D SiNWs at a probe wavelength of 715 nm at powers of 200, 125, 80, and 40 nJ/pulse following a 470 nm pump. Inset: Nonlinear power dependence of the maximum intensity of the signal as a function of pulse power following a 470 nm excitation and 715 nm probe.

fast component decreased superlinearly. Additionally, while the 200 nJ/pulse's fast decay component was 0.3 ps, the 125 and 80 nJ/pulse data had fast components of 0.5 and 1.8 ps, slow components of 6.9 and 8.6 ps, and long-time components of ~75 ps. Finally, for the lowest pump power of 40 nJ/pulse, the fast component disappeared, making the 40 nJ/pulse data a biexponential decay comprised solely of the two slow decay components with time constants of 9.2 and ~75 ps. Figure 4 and its inset also show that the amplitude of the fast component increases faster than that of the slower component with increased excitation intensities. For the reported lifetimes, a nominal error of ~10% is ascribed to the data.

PL spectroscopy indicated that the SiNWs are weakly luminescent. Two factors are responsible for high PL in nanostructured silicon: increased porosity,[33] and passivation of the surface with an oxide layer.[37] Studies have shown a dependence of PL intensity on the porosity of the silicon.[25,27] The stronger trap state emission from the porosity is associated with a net increase in the number of trap states. Therefore, more porous SiNWs can be expected to have increased trap state PL. However, passivation of the surface of the SiNWs with an oxide layer will lead to a decreased density of DT states, resulting in a net decrease in trap state PL intensity. Nevertheless, the PL that is observed (modeled in Figure 5) is believed to arise from the recombination from the Si/SiO_2 interface states, which act as DTs, for which this assignment has been made before.[19,20] SiNW samples with lower relative

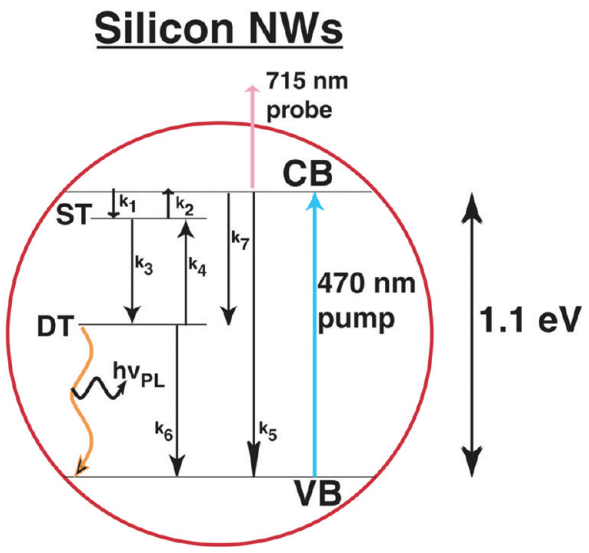

Figure 5. Proposed model for energy levels related to the optical properties and dynamics studies. CB and VB represent the conduction band and valence band, respectively, while ST represents shallow trap and DT stands for deep trap related to the $Si-SiO_2$ interface. At low power, the pump laser beam excites an electron from the VB into the CB, which is followed by nonradiative exciton decay or electron–hole recombination mediated by shallow and DT states. At high pump power, an additional, faster delay, attributed to exciton–exciton annihilation, takes place. The observed weak PL is attributed to radiative recombination from DT states related to the $Si-SiO_2$ interface.

porosity will thus have low overall PL, yet will exhibit characteristic SiO_2 peaks (Figure 2).

Our dynamics data show that the lifetime of the fast component decreases with increasing pump power (Figure 4). This is similar to what has been observed in previous studies of CdS quantum dots by Roberti et al.[38] With further increasing pump power, higher order kinetic processes can take place and result in faster decay or even shorter lifetime.[39−41] Nonlinear behaviors, such as exciton–exciton annihilation, occur when multiple excitons are generated where there is strong interaction between the excitons. This is typically reflected as an ultrafast dynamic process with a lifetime of hundreds of femtoseconds up to a few picoseconds and depends nonlinearly on the excitation light intensity.[39,41,42] The reported nonlinear decay kinetics can change considerably depending upon the system being studied. For example, TiO_2 nanoclusters have reported lifetimes of 0.5 ps,[43] AgI/Ag_2S core/shell particles with lifetimes of 0.8 ps,[44] and CdS quantum dots with lifetimes of 2.5 ps.[39]

In the meantime, the amplitude of the fast component grows more than linearly with increasing pump power (inset, Figure 4). The nonlinear increase in amplitude for the fast component with excitation intensity is also consistent with nonradiative exciton–exciton annihilation or Auger recombination, similar to what has been observed in other semiconductor nanostructures previously.[38,45−47] At low pump power, excitons generated can quickly dissociate into electrons and holes that can be trapped into trap states.[48,49] As the pump power is increased, an increased number of excitons are generated per particle or NW, which could generate enough electrons and holes to saturate the trap states. Upon saturation of the trap states, excitons can accumulate and exciton–exciton annihilation can occur, which is often reflected as a pump power-

dx.doi.org/10.1021/jz201597j | J. Phys. Chem. Lett. 2012, 3, 766–771

dependent fast decay in transient absorption measurements.[38,45] The slower 5 ps decay observed for SiNWs in this study is assigned to nonradiative recombination from trap states.[50] The recombination time is relatively short due to a high density of trap states that mediate the decay. Finally, the longer decay of ~75 ps is likely due to the presence of a high density of DT states or defect states.

Figure 5 is an energy model diagram for the SiNWs. After an initial 470 nm pump, a decay with an average of 5 ps occurs. Following that process, a slower 75 ps decay takes place. The faster 5 ps decay is attributable to nonradiative exciton decay or electron−hole recombination mediated by trap states occurring while a slower 75 ps decay related to deep trapping occurs. We believe the 75 ps component is related to the weak PL.

To gain further insight into the energy relaxation mechanism of the SiNWs, we utilized a four-state kinetic scheme to model the observed dynamics, as shown in Figure 5 and explained in more detail in the Supporting Information. The proposed scheme includes the VB, conduction band (CB), STs, and DTs. After combining the contributions of each of the states at varying percentages with a set of rate constants, we were able to closely model our experimental data. The rate constants were chosen based on the experimental results in this Letter as well as other experiments.[23,51−53]

In modeling the data for the SiNWs, the VB needs to be explicitly included since it is probed by the probe pulse and is reflected as a transient bleach signal. By combining 30% contribution from the VB, 30% from the CB, and 20% from both the STs and DTs, a curve could be generated that closely modeled our observed data. It should be noted that the model, as constructed, works for low laser power only. This is because adequate modeling at progressively higher powers would require an additional state to account for exciton−exciton annihilation, which is a second-order process.

In terms of the mechanism of the modeled decay, and from the final rate constants determined by comparing the modeled data with the experimental data, we are able to unambiguously assign rate constants to the key physical processes shown in Figure 5. In particular, the time constant from the CB to the ST was modeled to be 0.5 ps, while the decay from the ST to the DT is 4 ps and the DT to VB was 500 ps. Although the time constants may not be unique due to several assumptions made in the modeling scheme, we believe they are indicative of key physical processes that are occurring during the transient absorption decay profile.

In modeling the dynamics at low power, we discovered that the saturation of the STs results in accumulation of electrons in the CB. The result is that it increases the transient absorption over the bleach. Overall, this is most likely because the relaxation from the CB to the ST is an order of magnitude faster than that from the ST to the DT, and high-intensity excitation facilitates the accumulation of electrons in the ST states. This thereby leads to ST saturation more easily than that of DT. From modeling the individual states, we generated a series of plots that represent individual components that, when added, generate an overall curve that models the experimental data (Figure S1). Fitting the overall modeled curve with the same algorithm that fit the experimental data generated time constants, effectively allowing for a direct comparison between modeled and experimental data. From the modeled data, we obtained lifetime values of 0.48, 6.4, and 83 ps that support our experimental curve-fitting results with time constants of 0.3, 5, and ~75 ps. Any discrepancy is likely due to the model being a first-approximation. Nevertheless, both modeled as well as experimental data seem to reflect one another well.

Finally, in comparison to previous studies of high-power, nonlinear dynamical exciton dynamics of silicon nanoparticles[17,51,52,54] (SiNPs), the SiNWs seem to show a faster average decay time. Although rigorous quantitative comparisons are not easy since factors such as the laser power, spot size, and the surface conditions of the samples can be different and are important, faster exciton−exciton annihilation may be anticipated for SiNWs. This is because SiNWs are larger than typical SiNPs, and a stronger nonlinear effect is expected due to a higher number of excitons generated in one SiNW than in a SiNP, assuming the samples have similar optical density and similar surface properties in terms of density of trap states.[55]

Ultrafast exciton dynamics in SiNWs were studied using transient absorption pump−probe spectroscopy. A broad transient bleach was observed for probe wavelengths in the range of 500−770 nm following an initial excitation wavelength of 470 nm and can be fit to a triple exponential decay of 0.3, 5.4, and ~75 ps. The time constants were probe wavelength-independent, indicating broad absorption features of the transient species probed. Power dependence studies showed that the amplitude of the fast component increases superlinearly with increasing pump power, indicating a nonlinear process that is attributed to exciton−exciton annihilation upon trap state saturation. Despite the porosity of the sample, the surface passivation of the SiNWs with an oxide layer is believed to be critical in determining the threshold for observing exciton−exciton annihilation. Kinetic modeling of the relaxation mechanism of the SiNWs reinforced our experimental data fitting and also provided insight into the mechanism of the decay profile evolution of each of the states over time. The modeling determined that the relaxation from the CB to the ST occurred after 500 fs, while the ST-to-DT relaxation transition occurs with a time constant of 4 ps, and the DT-to-VB relaxation occurs with a time constant of 500 ps. These modeled findings are important in that they aid in assigning physical processes to time constants in the experimental data, helping unambiguously determine the major relaxation mechanism.

METHODS

SiNW Preparation. The SiNWs were synthesized by using electrochemical etching techniques following a previously reported synthetic protocol.[56] Briefly, a clean *n*-Si(100) wafer with 0.005−0.02 Ω·cm resistivity was immersed in a silver deposition solution containing 4.8 M HF and 0.005 M $AgNO_3$ for 1 min, and then etched in 4.8 M HF and 0.3 M H_2O_2 for 30 min. The dried SiNWs were cut off from the wafer and dispersed in approximately 100 μL of ethanol and sonicated for 30 min. Subsequently, 25 μL of the dispersed SiNWs were dried on a ZrO_2 film. The procedure was repeated once again to increase the SiNW film thickness until a yellow-brown color was observed.

UV−vis, Electron Microscopy (EM), and PL Measurements. UV−vis spectra of the dried, deposited SiNWs were collected using an HP 8452A diode array spectrophotometer with spectral resolution set at 2 nm. SEM was carried out using a Philips XL30 FEG microscope. HRTEM was performed on a Philips CM200-FEG. Porosity was measured using imageJ.[57] The PL spectra of the SiNWs were collected on a Renishaw InVia Raman microscope system using an excitation wavelength of 514.5 nm (Ar^+).

dx.doi.org/10.1021/jz201597j | J. Phys. Chem. Lett. 2012, 3, 766−771

Femtosecond Laser System and Transient Absorption Measurement. Ultrafast transient bleach measurements were conducted using an amplified femtosecond Ti-sapphire laser system described previously.[58] In all experiments, a pump wavelength of 470 nm was selected from an OPA (optical parametric amplifier) and used. In the wavelength-dependent study, an output pulse duration of <180 fs and a pulse energy of 200 nJ/pulse was used for all wavelengths used. A white light continuum (WLC) generated from a sapphire crystal was used as the probe pulse that was detected using a charge-coupled device (CCD) detector. Pump power-dependence studies were conducted with pump pulse energies of 200, 125, 80, and 40 nJ/pulse, which were varied using neutral density filters.

■ ASSOCIATED CONTENT

Supporting Information

Additional details regarding the kinetic modeling of charge carrier dynamics. This material is available free of charge via the Internet at http://pubs.acs.org.

■ AUTHOR INFORMATION

Corresponding Author

*E-mail: apannale@cityu.edu.hk (S.T.L.); zhang@ucsc.edu (J.Z.Z.). Phone: (831) 459-3776; Fax: (831) 459-2935.

Notes

The authors declare no competing financial interest.

■ ACKNOWLEDGMENTS

For J.Z.Z., this work was supported by the Basic Energy Sciences Division of the US DOE (DE-FG02-ER46232). S.T.L. was supported by the Research Grants Council of HKSAR (No. CityU101909 & CityU5/CRF/08).

■ REFERENCES

(1) Canham, L. T. Silicon Quantum Wire Array Fabrication by Electrochemical and Chemical Dissolution of Wafers. *Appl. Phys. Lett.* **1990**, *57*, 1046−1048.

(2) Li, Z.; Chen, Y.; Li, X.; Kamins, T. I.; Nauka, K.; Williams, R. S. Sequence-Specific Label-Free DNA Sensors Based on Silicon Nanowires. *Nano Lett.* **2004**, *4*, 245−247.

(3) Hahm, J.-i.; Lieber, C. M. Direct Ultrasensitive Electrical Detection of DNA and DNA Sequence Variations Using Nanowire Nanosensors. *Nano Lett.* **2003**, *4*, 51−54.

(4) Cui, Y.; Wei, Q.; Park, H.; Lieber, C. M. Nanowire Nanosensors for Highly Sensitive and Selective Detection of Biological and Chemical Species. *Science* **2001**, *293*, 1289−1292.

(5) Koo, S.-M.; Li, Q.; Edelstein, M. D.; Richter, C. A.; Vogel, E. M. Enhanced Channel Modulation in Dual-Gated Silicon Nanowire Transistors. *Nano Lett.* **2005**, *5*, 2519−2523.

(6) Cui, Y.; Zhong, Z.; Wang, D.; Wang, W. U.; Lieber, C. M. High Performance Silicon Nanowire Field Effect Transistors. *Nano Lett.* **2003**, *3*, 149−152.

(7) Duan, X.; Huang, Y.; Lieber, C. M. Nonvolatile Memory and Programmable Logic from Molecule-Gated Nanowires. *Nano Lett.* **2002**, *2*, 487−490.

(8) Huang, Y.; Duan, X.; Cui, Y.; Lauhon, L. J.; Kim, K.-H.; Lieber, C. M. Logic Gates and Computation from Assembled Nanowire Building Blocks. *Science* **2001**, *294*, 1313−1317.

(9) Kovalev, D.; Fuji, M. *Annual Review of Nano Research*; World Scientific: Singpore, 2008; Vol. *159*.

(10) Brus, L. Luminescence of Silicon Materials: Chains, Sheets, Nanocrystals, Nanowires, Microcrystals, and Porous Silicon. *J. Phys. Chem.* **1994**, *98*, 3575−3581.

(11) Allan, G.; Delerue, C. Efficient Intraband Optical Transitions in Si Nanocrystals. *Phys. Rev. B* **2002**, *66*, 233303−233306.

(12) Sa'ar, A.; Dovrat, M.; Jedrzejewski, J.; Balberg, I. Optical Inter- and Intra-Band Transitions in Silicon Nanocrystals: The Role of Surface Vibrations. *Phys. E (Amsterdam, Neth.)* **2007**, *38*, 122−127.

(13) Sa'ar, A.; Reichman, Y.; Dovrat, M.; Krapf, D.; Jedrzejewski, J.; Balberg, I. Resonant Coupling between Surface Vibrations and Electronic States in Silicon Nanocrystals at the Strong Confinement Regime. *Nano Lett.* **2005**, *5*, 2443−2447.

(14) Wolkin, M. V.; Jorne, J.; Fauchet, P. M.; Allan, G.; Delerue, C. Electronic States and Luminescence in Porous Silicon Quantum Dots: The Role of Oxygen. *Phys. Rev. Lett.* **1999**, *82*, 197−200.

(15) Kanemitsu, Y.; Suzuki, K.; Uto, H.; Masumoto, Y.; Matsumoto, T.; Kyushin, S.; Higuchi, K.; Matsumoto, H. Visible Photoluminescence of Silicon-Based Nanostructures: Porous Silicon and Small Silicon-Based Clusters. *Appl. Phys. Lett.* **1992**, *61*, 2446−2448.

(16) Malý, P.; Trojánek, F.; Hospodková, A.; Kohlová, V.; Pelant, I. Transmission Study of Picosecond Photocarrier Dynamics in Free-Standing Porous Silicon. *Solid State Commun.* **1994**, *89*, 709−712.

(17) Matsumoto, T.; Wright, O. B.; Futagi, T.; Mimura, H.; Kanemitsu, Y. Ultrafast Electronic Relaxation Processes in Porous Silicon. *J. Non-Cryst. Solids* **1993**, *164−166*, 953−956.

(18) Tsybeskov, L.; Vandyshev, J. V.; Fauchet, P. M. Blue Emission in Porous Silicon: Oxygen-Related Photoluminescence. *Phys. Rev. B* **1994**, *49*, 7821−7824.

(19) Dovrat, M.; Arad, N.; Zhang, X. H.; Lee, S. T.; Sa'ar, A. Optical Properties of Silicon Nanowires from Cathodoluminescence Imaging and Time-Resolved Photoluminescence Spectroscopy. *Phys. Rev. B* **2007**, *75*, 205343−205347.

(20) Dovrat, M.; Shalibo, Y.; Arad, N.; Popov, I.; Lee, S. T.; Sa'ar, A. Excitonic Transitions in Silicon Nanostructures Probed by Time-Resolved Photoluminescence Spectroscopy. *Phys. Status Solidi C* **2009**, *6*, 1615−1619.

(21) Dexheimer, S. L.; Zhang, C. P.; Liu, J.; Young, J. E.; Nelson, B. P. Ultrafast Carrier Thermalization in Hydrogenated Amorphous Silicon. *MRS Proc.* **2002**, *715*, A2.1.

(22) Myers, K. E.; Wang, Q.; Dexheimer, S. L. Ultrafast Carrier Dynamics in Nanocrystalline Silicon. *Phys. Rev. B* **2001**, *64*, 161309−161312.

(23) Trojánek, F.; Neudert, K.; Malý, P.; Dohnalová, K.; Pelant, I. Ultrafast Photoluminescence in Silicon Nanocrystals Studied by Femtosecond up-Conversion Technique. *J. Appl. Phys.* **2006**, *99*, 116108−116110.

(24) Kovalenko, S. A.; Dobryakov, A. L.; Karavanskii, V. A.; Lisin, D. V.; Merkulova, S. P.; Lozovik, Y. E. Femtosecond Spectroscopy of Porous Silicon. *Phys. Scr.* **1999**, *60*, 589−592.

(25) Klimov, V.; McBranch, D.; Karavanskii, V. Strong Optical Nonlinearities in Porous Silicon: Femtosecond Nonlinear Transmission Study. *Phys. Rev. B* **1995**, *52*, R16989−R16992.

(26) Klimov, V. I.; Dneprovskii, V. S.; Karavinskii, V. A. Nonlinear Transmission Spectra of Porous Silicon: Manifestation of Size Quantization. *Appl. Phys. Lett.* **1994**, *64*, 2691−2693.

(27) Van Dao, L.; Hannaford, P. Femtosecond Nonlinear Coherence Spectroscopy of Carrier Dynamics in Porous Silicon. *J. Appl. Phys.* **2005**, *98*, 083508−083512.

(28) Huang, Y.; Lieber, C. M. Integrated Nanoscale Electronics and Optoelectronics: Exploring Nanoscale Science and Technology through Semiconductor Nanowires. *Pure Appl. Chem.* **2004**, *76*, 2051−2068.

(29) Wang, D.; Wang, Q.; Javey, A.; Tu, R.; Dai, H.; Kim, H.; McIntyre, P. C.; Krishnamohan, T.; Saraswat, K. C. Germanium Nanowire Field-Effect Transistors with SiO_2 and High-k HfO_2 Gate Dielectrics. *Appl. Phys. Lett.* **2003**, *83*, 2432−2434.

(30) Patolsky, F.; Timko, B. P.; Yu, G.; Fang, Y.; Greytak, A. B.; Zheng, G.; Lieber, C. M. Detection, Stimulation, and Inhibition of Neuronal Signals with High-Density Nanowire Transistor Arrays. *Science* **2006**, *313*, 1100−1104.

(31) Tian, B.; Zheng, X.; Kempa, T. J.; Fang, Y.; Yu, N.; Yu, G.; Huang, J.; Lieber, C. M. Coaxial Silicon Nanowires As Solar Cells and Nanoelectronic Power Sources. *Nature* **2007**, *449*, 885−889.
(32) Chan, C. K.; Peng, H.; Liu, G.; McIlwrath, K.; Zhang, X. F.; Huggins, R. A.; Cui, Y. High-Performance Lithium Battery Anodes Using Silicon Nanowires. *Nat. Nanotechnol.* **2008**, *3*, 31−35.
(33) Lin, L.; Guo, S.; Sun, X.; Feng, J.; Wang, Y. Synthesis and Photoluminescence Properties of Porous Silicon Nanowire Arrays. *Nanoscale Res. Lett.* **2010**, *5*, 1822−1828.
(34) Beard, M. C.; Knutsen, K. P.; Yu, P.; Luther, J. M.; Song, Q.; Metzger, W. K.; Ellingson, R. J.; Nozik, A. J. Multiple Exciton Generation in Colloidal Silicon Nanocrystals. *Nano Lett.* **2007**, *7*, 2506−2512.
(35) Sivakov, V. A.; Voigt, F.; Berger, A.; Bauer, G.; Christiansen, S. H. Roughness of Silicon Nanowire Sidewalls and Room Temperature Photoluminescence. *Phys. Rev. B 82*, 125446-125451.
(36) Zhang, X.; Tian, H.; He, J.; Fang, X. Spectroscopic Changes of Silicon Nanowires Induced by Femtosecond Laser Pulses. *Chem. Lett.* **2010**, *39*, 890−891.
(37) Shih, S.; Jung, K.; Yan, J.; Kwong, D.; Kovar, M.; White, J.; George, T.; Kim, S. Photoinduced Luminescence Enhancement from Anodically Oxidized Porous Si. *Appl. Phys. Lett.* **1993**, *63*, 3306−3308.
(38) Roberti, T.; Cherepy, N.; Zhang, J. TI - Nature of the Power-Dependent Ultrafast Relaxation Process of Photoexcited Charge Carriers in II−VI Semiconductor Quantum Dots: Effects of Particle Size, Surface, and Electronic Structure. *J. Chem. Phys.* **1998**, *108*, 2143−2151.
(39) Zhang, J. Z.; O'Neil, R. H.; Roberti, T. W. Femtosecond Studies of Photoinduced Electron Dynamics at the Liquid-Solid Interface of Aqueous CdS Colloids. *J. Phys. Chem.* **1994**, *98*, 3859−3864.
(40) Xu, X.; Zhao, Y.; Sie, E. J.; Lu, Y.; Liu, B.; Ekahana, S. A.; Ju, X.; Jiang, Q.; Wang, J.; Sun, H.; Sum, T. C.; Huan, C.; et al. Dynamics of Bound Exciton Complexes in CdS Nanobelts. *ACS Nano* **2011**, *5*, 3660−3669.
(41) Wheeler, D.; Fitzmorris, B.; Zhao, H.; Ma, D.; Zhang, J. Ultrafast Exciton Relaxation Dynamics of PbS and Core/Shell PbS/CdS Quantum Dots. *Sci. China, Ser. B: Chem.* **2011**, *54*, 2009−2015.
(42) Skinner, D. E.; Colombo, D. P.; Cavaleri, J. J.; Bowman, R. M. Femtosecond Investigation of Electron Trapping in Semiconductor Nanoclusters. *J. Phys. Chem.* **1995**, *99*, 7853−7856.
(43) Philip Colombo, D. Jr; Roussel, K. A.; Saeh, J.; Skinner, D. E.; Cavaleri, J. J.; Bowman, R. M. Femtosecond Study of the Intensity Dependence of Electron-Hole Dynamics in TiO_2 Nanoclusters. *Chem. Phys. Lett.* **1995**, *232*, 207−214.
(44) Brelle, M. C.; Zhang, J. Z. Femtosecond Study of Photo-induced Electron Dynamics in AgI and Core/Shell Structured AgI/Ag_2S and AgBr/Ag_2S Colloidal Nanoparticles. *J. Chem Phys.* **1998**, *108*, 3119−3126.
(45) Zheng, J.; Kwok, H. Exciton and Biexciton Recombination in Semiconductor Nanocrystals. *Appl. Phys. Lett.* **1994**, *65*, 1151−1153.
(46) Burda, C.; Link, S.; Mohamed, M.; El-Sayed, M. The Pump Power Dependence of the Femtosecond Relaxation of CdSe Nanoparticles Observed in the Spectral Range from Visible to Infrared. *J. Chem. Phys.* **2002**, *116*, 3828−3833.
(47) Burda, C.; Link, S.; Green, T. C.; El-Sayed, M. A. New Transient Absorption Observed in the Spectrum of Colloidal CdSe Nanoparticles Pumped with High-Power Femtosecond Pulses. *J. Phys. Chem. B* **1999**, *103*, 10775−10780.
(48) Thibert, A. J.; Frame, F. A.; Busby, E.; Larsen, D. S. Primary Photodynamics of Water Solubilized Two-Dimensional CdSe Nanoribbons. *J. Phys. Chem. C* **2011**, *115*, 19647−19658.
(49) Liu, R.; Chen, Y.; Wang, F.; Cao, L.; Pan, A.; Yang, G.; Wang, T.; Zou, B. Stimulated Emission from Trapped Excitons in SnO_2 Nanowires. *Phys. E (Amsterdam, Neth.)* **2007**, *39*, 223−229.
(50) Grant, C. D.; Zhang, J. Z. *Annual Review of Nano Research*; World Scientific Publisher: Singapore, 2008; Vol. 2.
(51) Kuntermann, V.; Cimpean, C.; Brehm, G.; Sauer, G.; Kryschi, C.; Wiggers, H. Femtosecond Transient Absorption Spectroscopy of Silanized Silicon Quantum Dots. *Phys. Rev. B* **2008**, *77*, 115343−115350.
(52) Cimpean, C.; Groenewegen, V.; Kuntermann, V.; Sommer, A.; Kryschi, C. Ultrafast Exciton Relaxation Dynamics in Silicon Quantum Dots. *Laser Photonics Rev.* **2009**, *3*, 138−145.
(53) Owrutsky, J. C.; Rice, J. K.; Guha, S.; Steiner, P.; Lang, W. Ultrafast Absorption in Free-Standing Porous Silicon Films. *Appl. Phys. Lett.* **1995**, *67*, 1966−1968.
(54) Klimov, V.; Schwarz, C.; McBranch, D.; White, C. Initial Carrier Relaxation Dynamics in Ion-Implanted Si Nanocrystals: Femtosecond Transient Absorption Study. *Appl. Phys. Lett.* **1998**, *73*, 2603−2605.
(55) Wu, F.; Yu, J. H.; Joo, J.; Hyeon, T.; Zhang, J. Z. Ultrafast Electronic Dynamics of Monodisperse PbS and CdS Nanoparticles/Nanorods: Effects of Size on Nonlinear Relaxation. *Opt. Mater.* **2007**, *29*, 858−866.
(56) Zhang, M.-L.; Peng, K.-Q.; Fan, X.; Jie, J.-S.; Zhang, R.-Q.; Lee, S.-T.; Wong, N.-B. Preparation of Large-Area Uniform Silicon Nanowires Arrays through Metal-Assisted Chemical Etching. *J. Phys. Chem. C* **2008**, *112*, 4444−4450.
(57) Rasband, W. S. *ImageJ*; U.S. National Institute of Health: Bethesda, MD, 1997−2009 (http://rsb.info.nih.gov/ij/).
(58) Newhouse, R. J.; Wang, H.; Hensel, J. K.; Wheeler, D. A.; Zou, S.; Zhang, J. Z. Coherent Vibrational Oscillations of Hollow Gold Nanospheres. *J. Phys. Chem. Lett.* **2011**, *2*, 228−235.